Search for $B \to \ell \bar{\nu}_\ell$

M. Artuso,[1] M. Gao,[1] M. Goldberg,[1] D. He,[1] N. Horwitz,[1] G. C. Moneti,[1] R. Mountain,[1] F. Muheim,[1] Y. Mukhin,[1] S. Playfer,[1] Y. Rozen,[1] S. Stone,[1] X. Xing,[1] G. Zhu,[1] J. Bartelt,[2] S. E. Csorna,[2] Z. Egyed,[2] V. Jain,[2] D. Gibaut,[3] K. Kinoshita,[3] P. Pomianowski,[3] B. Barish,[4] M. Chadha,[4] S. Chan,[4] D. F. Cowen,[4] G. Eigen,[4] J. S. Miller,[4] C. O'Grady,[4] J. Urheim,[4] A. J. Weinstein,[4] F. Würthwein,[4] D. M. Asner,[5] M. Athanas,[5] D. W. Bliss,[5] W. S. Brower,[5] G. Masek,[5] H. P. Paar,[5] J. Gronberg,[6] C. M. Korte,[6] R. Kutschke,[6] S. Menary,[6] R. J. Morrison,[6] S. Nakanishi,[6] H. N. Nelson,[6] T. K. Nelson,[6] C. Qiao,[6] J. D. Richman,[6] D. Roberts,[6] A. Ryd,[6] H. Tajima,[6] M. S. Witherell,[6] R. Balest,[7] K. Cho,[7] W. T. Ford,[7] M. Lohner,[7] H. Park,[7] P. Rankin,[7] J. G. Smith,[7] J. P. Alexander,[8] C. Bebek,[8] B. E. Berger,[8] K. Berkelman,[8] K. Bloom,[8] T. E. Browder,[8,*] D. G. Cassel,[8] H. A. Cho,[8] D. M. Coffman,[8] D. S. Crowcroft,[8] M. Dickson,[8] P. S. Drell,[8] D. J. Dumas,[8] R. Ehrlich,[8] R. Elia,[8] P. Gaidarev,[8] R. S. Galik,[8] M. Garcia-Sciveres,[8] B. Gittelman,[8] S. W. Gray,[8] D. L. Hartill,[8] B. K. Heltsley,[8] S. Henderson,[8] C. D. Jones,[8] S. L. Jones,[8] J. Kandaswamy,[8] N. Katayama,[8] P. C. Kim,[8] D. L. Kreinick,[8] Y. Liu,[8] G. S. Ludwig,[8] J. Masui,[8] J. Mevissen,[8] N. B. Mistry,[8] C. R. Ng,[8] E. Nordberg,[8] J. R. Patterson,[8] D. Peterson,[8] D. Riley,[8] A. Soffer,[8] P. Avery,[9] A. Freyberger,[9] K. Lingel,[9] J. Rodriguez,[9] S. Yang,[9] J. Yelton,[9] G. Brandenburg,[10] D. Cinabro,[10] T. Liu,[10] M. Saulnier,[10] R. Wilson,[10] H. Yamamoto,[10] T. Bergfeld,[11] B. I. Eisenstein,[11] J. Ernst,[11] G. E. Gladding,[11] G. D. Gollin,[11] M. Palmer,[11] M. Selen,[11] J. J. Thaler,[11] K. W. Edwards,[12] K. W. McLean,[12] M. Ogg,[12] A. Bellerive,[13] D. I. Britton,[13] E. R. F. Hyatt,[13] R. Janicek,[13] D. B. MacFarlane,[13] P. M. Patel,[13] B. Spaan,[13] A. J. Sadoff,[14] R. Ammar,[15] P. Baringer,[15] A. Bean,[15] D. Besson,[15] D. Coppage,[15] N. Copty,[15] R. Davis,[15] N. Hancock,[15] M. Kelly,[15] S. Kotov,[15] I. Kravchenko,[15] N. Kwak,[15] H. Lam,[15] Y. Kubota,[16] M. Lattery,[16] M. Momayezi,[16] J. K. Nelson,[16] S. Patton,[16] R. Poling,[16] V. Savinov,[16] S. Schrenk,[16] R. Wang,[16] M. S. Alam,[17] I. J. Kim,[17] Z. Ling,[17] A. H. Mahmood,[17] J. J. O'Neill,[17] H. Severini,[17] C. R. Sun,[17] F. Wappler,[17] G. Crawford,[18] R. Fulton,[18] D. Fujino,[18] K. K. Gan,[18] K. Honscheid,[18] H. Kagan,[18] R. Kass,[18] J. Lee,[18] M. Sung,[18] C. White,[18] A. Wolf,[18] M. M. Zoeller,[18] X. Fu,[19] B. Nemati,[19] W. R. Ross,[19] P. Skubic,[19] M. Wood,[19] M. Bishai,[20] J. Fast,[20] E. Gerndt,[20] J. W. Hinson,[20] R. L. McIlwain,[20] T. Miao,[20] D. H. Miller,[20] M. Modesitt,[20] D. Payne,[20] E.I. Shibata,[20] I. P. J. Shipsey,[20] P. N. Wang,[20] L. Gibbons,[21] Y. Kwon,[21] S. Roberts,[21] E. H. Thorndike,[21] T. Coan,[22] J. Dominick,[22] V. Fadeyev,[22] I. Korolkov,[22] M. Lambrecht,[22] S. Sanghera,[22] V. Shelkov,[22] T. Skwarnicki,[22] R. Stroynowski,[22] I. Volobouev,[22] and G. Wei[22]

(CLEO Collaboration)

[1]*Syracuse University, Syracuse, New York 13244*
[2]*Vanderbilt University, Nashville, Tennessee 37235*
[3]*Virginia Polytechnic Institute and State University, Blacksburg, Virginia 24061*
[4]*California Institute of Technology, Pasadena, California 91125*
[5]*University of California, San Diego, La Jolla, California 92093*
[6]*University of California, Santa Barbara, California 93106*
[7]*University of Colorado, Boulder, Colorado 80309-0390*
[8]*Cornell University, Ithaca, New York 14853*
[9]*University of Florida, Gainesville, Florida 32611*
[10]*Harvard University, Cambridge, Massachusetts 02138*
[11]*University of Illinois, Champaign-Urbana, Illinois 61801*
[12]*Carleton University, Ottawa, Ontario, Canada K1S 5B6*
and The Institute of Particle Physics, Montréal, Québec, Canada
[13]*McGill University, Montréal, Québec, Canada H3A 2T8*
and The Institute of Particle Physics, Montréal, Québec, Canada
[14]*Ithaca College, Ithaca, New York 14850*
[15]*University of Kansas, Lawrence, Kansas 66045*
[16]*University of Minnesota, Minneapolis, Minnesota 55455*
[17]*State University of New York at Albany, Albany, New York 12222*
[18]*The Ohio State University, Columbus, Ohio 43210*
[19]*University of Oklahoma, Norman, Oklahoma 73019*
[20]*Purdue University, West Lafayette, Indiana 47907*
[21]*University of Rochester, Rochester, New York 14627*
[22]*Southern Methodist University, Dallas, Texas 75275*
(Received 31 March 1995)

0031-9007/95/75(5)/785(5)$06.00

We search for the decays $B^- \to \ell^- \bar{\nu}_\ell$ in a sample of 2.2×10^6 charged B decays using the CLEO detector. We see no evidence for a signal in any channel and set upper limits on the branching fractions of $\mathcal{B}(B^- \to \tau^- \bar{\nu}_\tau) < 2.2 \times 10^{-3}$, $\mathcal{B}(B^- \to \mu^- \bar{\nu}_\mu) < 2.1 \times 10^{-5}$, and $\mathcal{B}(B^- \to e^- \bar{\nu}_e) < 1.5 \times 10^{-5}$ at the 90% confidence level.

PACS numbers: 13.20.He, 14.80.Cp

In the standard model, the exclusive decays of charged mesons to a lepton plus its neutrino proceed primarily through the annihilation of the constituent quarks in the meson into a virtual W boson. For the B meson, this branching fraction is given by

$$\mathcal{B}(B \to \ell \bar{\nu}_\ell) = \frac{G_F^2 m_B m_\ell^2}{8\pi}\left(1 - \frac{m_\ell^2}{m_B^2}\right)^2 f_B^2 |V_{ub}|^2 \tau_B, \quad (1)$$

where ℓ represents e, μ, or τ, G_F is the Fermi coupling constant, m_B and m_ℓ are the meson and lepton masses, τ_B is the B meson lifetime, V_{ub} is the Cabibbo-Kobayashi-Maskawa quark mixing matrix element, and f_B is the decay constant, which parametrizes the overlap of the quark wave functions within the meson. (Throughout this paper $B \to \ell \bar{\nu}_\ell$ refers to both $B^- \to \ell^- \bar{\nu}_\ell$ and $B^+ \to \ell^+ \nu_\ell$.) A measurement of this branching fraction would provide valuable new information on quark mixing through the product $f_B|V_{ub}|$, since the values of the other parameters are comparatively well known [1]. The expected value of $\mathcal{B}(B \to \tau \bar{\nu}_\tau)$ lies in the range $(1 - 10) \times 10^{-5}$, while those of $\mathcal{B}(B \to \mu \bar{\nu}_\mu)$ and $\mathcal{B}(B \to e \bar{\nu}_e)$ are smaller by factors of 225 and 9.5×10^6, respectively, because of helicity suppression. The decay $B \to \ell \bar{\nu}_\ell$ also probes physics outside the standard model [2–4]. For example, the decay could proceed through the annihilation of the b and $\bar{u}$ quarks into a charged Higgs particle as predicted by certain supersymmetric models. Such a mechanism could enhance the $B \to \ell \bar{\nu}_\ell$ decay rates significantly. In this Letter, we describe searches for the decays $B \to \tau \bar{\nu}_\tau$, $B \to \mu \bar{\nu}_\mu$, and $B \to e \bar{\nu}_e$. A limit on $B \to \tau \bar{\nu}$ has recently been reported by the ALEPH experiment [5]; this is the first search for $B \to \mu \bar{\nu}_\mu$ and $B \to e \bar{\nu}_e$.

We search for events in which there is a single, well-identified lepton and the remaining particles are consistent with the decay of a second B. The latter constraint is enforced by requiring that $M \equiv (E_{\text{beam}}^2 - |\vec{p}_2|^2)^{1/2}$ is close to the B meson mass and $\Delta E \equiv E_2 - E_{\text{beam}}$ is consistent with zero, where $|\vec{p}_2|$ (E_2) is the net momentum (energy) of all detected particles except the lepton. In the case of the two-body $B \to \mu \bar{\nu}_\mu$ and $B \to e \bar{\nu}_e$ decays, the lepton energy is approximately $m_B/2$, where m_B is the B meson mass. In $B \to \tau \bar{\nu}_\tau$ decays followed by the leptonic tau decay $\tau \to e(\mu) \bar{\nu}_{e(\mu)} \nu_\tau$, the momentum of the observed lepton is not fixed. Because the absence of this constraint changes the analysis considerably, the $B \to \tau \bar{\nu}_\tau$ and $B \to \mu(e) \bar{\nu}_{\mu(e)}$ cases are discussed separately below.

The data used in this search were collected with the CLEO detector operating at the Cornell Electron Storage Ring (CESR), and consist of approximately 2.2×10^6 $\Upsilon(4S) \to B\bar{B}$ events collected along with 6.8×10^6 ($e^+e^- \to q\bar{q}$) plus other continuum events at the $\Upsilon(4S)$ resonance at $\sqrt{s} = 10.58$ GeV (the "on-resonance" sample). These B mesons have momenta of 320 MeV/c. We also use a sample of 3.4×10^6 ($e^+e^- \to q\bar{q}$) plus other continuum events collected below resonance at $\sqrt{s} = 10.52$ GeV for background subtraction (the "off-resonance" sample).

The relevant features of the CLEO detector [6] are described here. The trajectories of charged particles are reconstructed using a system of three concentric wire chambers covering 95% of 4π in an axial magnetic field of 1.5 T. A CsI electromagnetic calorimeter covering 98% of 4π detects photons with energies above 30 MeV. Electrons are identified using the momentum-energy balance of tracks matched to showers in the calorimeter and their specific ionization in the drift chamber. Muons are identified by their penetration through the steel surrounding the magnetic coil. Other charged particles are identified through their specific ionization (dE/dx) in the main drift chamber. When calculating the energies of charged particles, all are assigned the pion mass unless they are identified as leptons or their dE/dx is inconsistent with the pion hypothesis ($>2\sigma$) and consistent with either the kaon or proton mass hypothesis ($<2\sigma$). There is no hadron calorimeter.

Consider first the search for $B \to \tau \bar{\nu}_\tau$. We select hadronic events by requiring that there be at least 4 charged tracks and significant visible energy. Continuum backgrounds are suppressed by requiring that $|\cos\theta_{\text{miss}}| < 0.95$, where θ_{miss} is the angle between the missing momentum and the beam line. To further suppress continuum decays, we select events that are spherical in shape by requiring that the ratio of the second and zeroth Fox-Wolfram moments [7] (R_2) be less than 0.50. We reduce the contribution from $e^+e^- \to \tau^+\tau^-$ and $e^+e^-\gamma\gamma$ events by requiring that $E_\ell + E_2 > E_{\text{beam}}$. To suppress events in which charged particles were lost we require the sum of the charges of the tracks, $\sum Q$, to be zero. Finally, we select events with exactly one identified e or μ, which we attribute to the tau decay.

At this stage we calculate M and ΔE. Our result is determined from a fit by this two-dimensional distribution; however, quoted yields and efficiencies refer to a signal region defined as $M > 5.27$ GeV and $-2 \le \Delta E < 0$ GeV. We find a total of 968 events from the on-resonance sample in this signal region. After subtracting continuum events using the scaled off-resonance sample,

651 ± 40 events remain. The probability that an event in which $B \to \tau\bar{\nu}_\tau$ followed by $\tau \to e(\mu)\bar{\nu}_{e(\mu)}\nu_\tau$ satisfies all selection criteria and lies in the signal region has been determined using a Monte Carlo simulation with corrections described below and is (4.1 ± 0.2)%, where the error is statistical only.

The lepton in most events in the signal region is the product of semileptonic B decay (90%), with smaller contributions from the secondary decay $b \to Xc \to Y\ell\bar{\nu}_\ell$ (7%) and hadrons misidentified as leptons (1%). These events enter the signal region only if 3–4 GeV of energy is undetected, usually because of extra neutrinos (67% of events) or neutral hadrons, or both. In 83% of the background events, the energy missed due to neutral hadrons exceeds 500 MeV. Only 14% of the signal events have this problem. Usually, neutral hadronic energy is missed because of K_L mesons that shower only partially or not at all in the CsI calorimeter.

We fit for the normalizations of three event samples: the $B \to \tau\bar{\nu}_\tau$ signal, the $B\bar{B}$ background in which at least one B has decayed semileptonically, and the $B\bar{B}$ background in which the lepton comes from the secondary decay ($b \to Xc \to Y\ell\bar{\nu}_\ell$) or a missed pair conversion, or is a hadron that has been mistaken for a lepton. We take the shapes of these three distributions from a Monte Carlo simulation. There are 60 011 ± 364 events in the fit region after subtraction of the scaled continuum.

Figures 1 and 2 show the ΔE and M distributions, respectively. A lego plot of the two-dimensional distribution can be seen in Ref. [8]. The quality of the two-dimensional fit is very good, with a χ^2 of 271 for 267 degrees of freedom, and the resulting normalizations of the background distributions agree well with the absolute predictions based on luminosity and the $B\bar{B}$ cross section and branching fractions. The number of signal events found in the signal region is −9 ± 36, where the error is statistical only. Figure 3(a) shows the distribution of p^*_ℓ, the lepton momentum in the rest frame of the parent B, for the data and the Monte Carlo, calculated assuming that the B direction is given by $-\vec{p}_2$ and that its momentum is 320 MeV/c. The Monte Carlo simulated background again agrees well with the data.

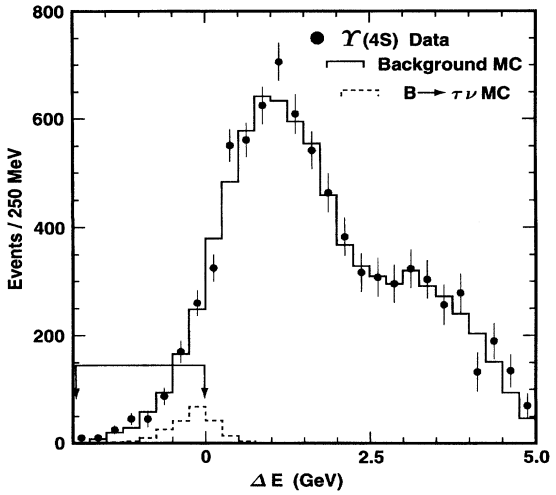

FIG. 1. The ΔE distribution for the $B \to \tau\bar{\nu}$ analysis after all other cuts including $M > 5.27$ GeV. The data (filled circles) are shown after the subtraction of scaled off-resonance events; the Monte Carlo simulated background is indicated by the histogram. The $\tau\bar{\nu}_\tau$ Monte Carlo simulated signal (dashed histogram) is shown with normalization appropriate for a branching fraction of 5.0×10^{-3}. The fit is limited to the region $-2.0 \le \Delta E < 2.5$ GeV, and the signal region is indicated by the arrows.

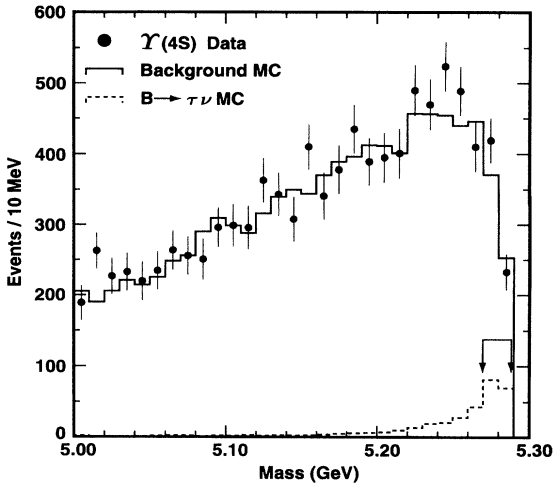

FIG. 2. The beam-constrained mass distribution for the $B \to \tau\bar{\nu}$ analysis after all other cuts including $-2.0 < \Delta E < 0.0$ GeV. The data (filled circles) are shown after the subtraction of scaled off-resonance events; the Monte Carlo simulated background is indicated by the histogram. The $\tau\bar{\nu}_\tau$ Monte Carlo simulated signal (dashed histogram) is shown with normalization appropriate for a branching fraction of 5.0×10^{-3}. The fit is limited to the region $5.15 \le M < 5.3$ GeV, and the signal region is indicated by the arrows.

The signal efficiency is initially determined using a Monte Carlo simulation and is then checked with independent data samples and corrected where necessary. In particular, the probability that only one lepton is observed is extracted from the number distribution of leptons in $B\bar{B}$ events, and the requirement that the net charge be zero is checked using events outside the fit region.

The systematic uncertainty in the signal efficiency is dominated by uncertainty in the M vs ΔE distribution. To evaluate this, we calculate M and ΔE using the remaining particles in events in which one of the two B decays has been fully reconstructed. These distributions are shown in Fig. 4 for a subsample of these events in which the reconstructed decay is $B \to D^*\ell\bar{\nu}$. The systematic error is assumed to be bounded by the change in the yield when we modify the signal distribution by amounts consistent with these data. The net systematic error due

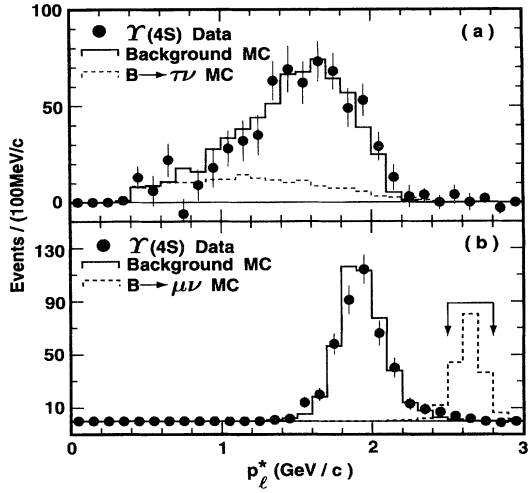

FIG. 3. (a) The distribution of p_ℓ^* for the $B \to \tau\bar{\nu}_\tau$ analysis after all cuts have been applied. The filled circles show the data after the subtraction of the scaled off-resonance sample, the histogram shows the Monte Carlo simulated background, and the dashed histogram shows the $\tau\bar{\nu}_\tau$ Monte Carlo simulated signal with normalization appropriate for a branching fraction of 5.0×10^{-3}. (b) The distribution of p_ℓ^* for the $B \to \mu\bar{\nu}_\mu$ analysis after all other cuts have been applied. The $\mu\bar{\nu}_\mu$ signal Monte Carlo is shown with normalization appropriate for a branching fraction of 5.0×10^{-4}. The accepted region is indicated by the arrows.

to uncertainty in the signal efficiency is dominated by the statistics of these studies, and is $\pm 9.0\%$.

To quantify the systematic uncertainty due to mismodeling of the background we measure the change in the signal yield when we vary parameters of the background simulation. These studies are summarized in Table I. Reasonable variation in K_L production is determined using reconstructed K_S's while variation in the energy deposited by K_L's in the calorimeter is determined from studies of the showers of charged kaons. We add the tabulated results in quadrature to find a total systematic uncertainty due to simulation of the background of ± 27 events.

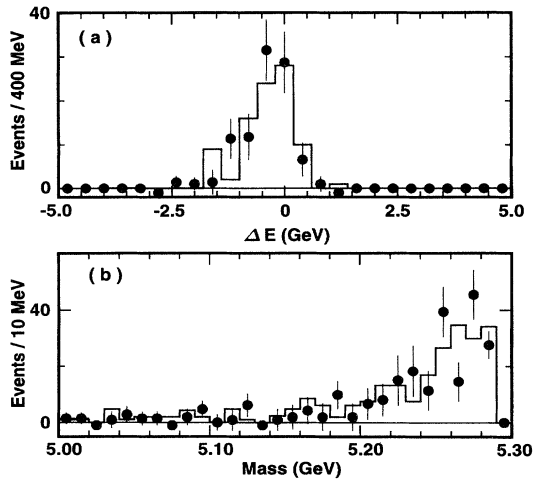

FIG. 4. The distributions of (a) ΔE and (b) M, for the $B \to D^*\ell\bar{\nu}_\ell$ sample after all other cuts for the $B \to \tau\bar{\nu}$ analysis except $\sum Q = 0$ have been applied. The circles are the data, and the histogram is the Monte Carlo normalized to the data using the number of reconstructed $D^*\ell\bar{\nu}_\ell$ decays.

TABLE I. Systematic uncertainties in the simulation of the $B \to \tau\bar{\nu}_\tau$ background.

	Variation	Change in result (events)
$\mathcal{B}(b \to Xc \to Y\ell\bar{\nu}_\ell)$ [9] around 9.25%	$\pm 1.39\%$	∓ 17
$b \to Xc \to Y\ell\bar{\nu}_\ell$ lepton energy	± 25 MeV	± 15
Neutral kaon production	$\pm 5\%$	∓ 12
$\mathcal{B}(B \to X\tau\bar{\nu}_\tau)$ around 2.5%	$\pm 0.5\%$	∓ 6
Detected energy per neutral kaon	$\pm 6.0\%$	± 4
Fraction of hadrons mistaken for leptons	$\pm 50\%$	± 1
Total		± 27

In addition to the uncertainties mentioned above, there is an uncertainty of $\pm 1.8\%$ in the number of B^+B^- events in our data sample and of 0.9% in $\mathcal{B}(\tau \to \ell\nu_\tau\bar{\nu}_\ell)$ [10]. We find a central value for the branching fraction of $(-0.3 \pm 1.4) \times 10^{-3}$. To determine an upper limit on the branching fraction, we simulate a large number of experiments with different values of the branching fraction. For each simulated experiment, we draw a signal efficiency and background level from Gaussian distributions and use them to generate a signal yield, which we compare with our central value of -9 events. The 90% confidence limit is that value of the true branching fraction which yields -9 events or fewer 10% as often as does a true branching fraction of zero. We find

$$\mathcal{B}(B \to \tau\bar{\nu}_\tau) < 2.2 \times 10^{-3} \quad (2)$$

at the 90% confidence level. Other approaches for obtaining a limit give similar results.

Now consider the searches for $B \to \mu\bar{\nu}_\mu$ and $B \to e\bar{\nu}_e$. We start with the data sample used above for the $B \to \tau\bar{\nu}_\tau$ search. Because the $\mu\bar{\nu}_\mu$ and $e\bar{\nu}_e$ channels are two-body decays, the daughter leptons have fixed momentum in the B rest frame, $p_\ell^* = 2.645$ GeV/c. We therefore require $2.545 \le p_\ell^* < 2.745$ GeV/c. This constraint eliminates essentially all $b \to c\ell\bar{\nu}_\ell$ background, leaving only continuum and $b \to u\ell\bar{\nu}_\ell$ events. Then to increase the signal yield, we relax the constraints on $B\bar{B}$ topology using instead $M > 5.23$ GeV and $-2 \le \Delta E < 0.5$ GeV, and we lift the requirement on $\sum Q$. These selection criteria are 28% (25%) efficient for $B \to \mu\bar{\nu}_\mu$ ($e\bar{\nu}_e$) Monte Carlo simulated signal events.

The next step is to reduce the background from continuum events in which a hadron is mistaken for a μ or e. First we take advantage of the large momentum of the lepton and impose more stringent identification requirements:

deeper penetration of the steel for muons, closer match between momentum and energy and to the expected dE/dx for electrons, and restricting both to the central part of the detector. For further reduction of the continuum background we make use of its collimated topology by tightening the requirement on R_2 from 0.5 to 0.3 and by rejecting events in which the lepton trajectory is collinear with the thrust axis of the rest of the event: $|\cos\theta_{\ell-\text{thrust}}| < 0.7$. The combination of these requirements eliminates approximately 95% of the remaining continuum background while reducing the $\mu\bar{\nu}_\mu$ ($e\bar{\nu}_e$) signal by only 48% (53%). The probability that an event with a $B \to \mu\bar{\nu}_\mu$ or $e\bar{\nu}_e$ decay satisfies all selection criteria is $(13 \pm 1)\%$ in both cases, where the error is evaluated as for the $B \to \tau\bar{\nu}_\tau$ analysis.

After applying all selection criteria we observe 3 (2) events in the $\mu\bar{\nu}_\mu$ ($e\bar{\nu}_e$) sample. The size of the remaining continuum background in the on-resonance data sample is then estimated using the off-resonance data sample, which is a factor of 2 smaller. Using the same selection criteria as for the on-resonance sample except for a 4 times larger p_ℓ^* window, we estimate that the number of continuum events remaining in the $\mu\bar{\nu}_\mu$ ($e\bar{\nu}_e$) sample is 1.5 ± 0.9 (2.5 ± 1.1). We estimate that the background from $b \to c\ell\bar{\nu}_\ell$ processes is negligible; however, assuming that $|V_{ub}/V_{cb}|^2 = 0.008$ we find an estimated background of 0.4 ± 0.2 events from $b \to u\ell\bar{\nu}_\ell$ processes. The p_ℓ^* distribution for the on-resonance data with the scaled off-resonance data subtracted is shown in Fig. 3(b) after all $B \to \mu\bar{\nu}_\mu$ selection criteria have been imposed. The figure also includes curves for the Monte Carlo simulations of the $\mu\bar{\nu}_\mu$ signal and the $B\bar{B}$ background.

In order to calculate upper limits on the possible number of signal events that have been observed we conservatively reduce the combined background estimates given above by one standard deviation to 1.0 (1.8) event for $\mu\bar{\nu}_\mu$ ($e\bar{\nu}_e$). Assuming these background estimates to be fixed parameters and combining them with the observed number of events in the signal samples we find upper limits at the 90% confidence level of 5.7 $B \to \mu\bar{\nu}_\mu$ and 4.0 $B \to e\bar{\nu}_e$ events. In order to calculate branching ratio limits we reduce the estimated signal selection efficiency by one standard deviation to 12% and obtain

$$\mathcal{B}(B \to \mu\bar{\nu}_\mu) < 2.1 \times 10^{-5}, \quad (3)$$

$$\mathcal{B}(B \to e\bar{\nu}_e) < 1.5 \times 10^{-5}. \quad (4)$$

The limit on $B \to \tau\bar{\nu}_\tau$ implies that the product $f_B|V_{ub}|$ is less than 3.6 MeV with 90% confidence. It also rules out the existence of a charged Higgs particle with small mass and large $\tan\beta$ in models with two Higgs doublets in which the u-type and d-type quarks acquire their masses from different Higgs particles (model II). Following Hou [3], we find $m_H > (2.0\ \text{GeV})\tan\beta \times [f_B/(200\ \text{MeV})]^{1/2}(V_{ub}/0.003)^{1/2}$. Somewhat weaker constraints result from the limit on $B \to \mu\bar{\nu}_\mu$.

We gratefully acknowledge the effort of the CESR staff in providing us with excellent luminosity and running conditions. This work was supported by the National Science Foundation, the U.S. Department of Energy, the Heisenberg Foundation, the Alexander von Humboldt Stiftung, the Natural Sciences and Engineering Research Council of Canada, and the A.P. Sloan Foundation.

*Permanent address: University of Hawaii at Manoa, Honolulu, HI 96822.

[1] L. Montanet *et al.*, Phys. Rev. D **50**, 51 (1994).
[2] E. Eichten *et al.*, Phys. Rev. D **34**, 1547 (1986).
[3] W-S. Hou, Phys. Rev. D **48**, 2342 (1993).
[4] G. Valencia and S. Willenbrook, Phys. Rev. D **50**, 6843 (1994).
[5] ALEPH Collaboration, D. Buskulic *et al.*, Phys. Lett. B **343**, 444 (1995).
[6] CLEO Collaboration, Y. Kubota *et al.*, Nucl. Instrum. Methods Phys. Res., Sect. A **320**, 66 (1992).
[7] G. Fox and S. Wolfram, Phys. Rev. Lett. **41**, 1581 (1978).
[8] CLEO Collaboration, J.P. Alexander *et al.*, Report No. ICHEP94 GLS0160 or No. CLEO CONF 94-5.
[9] A preliminary result was given in CLEO Collaboration, J. Gronberg *et al.*, Report No. ICHEP94 GLS0741 or No. CLEO CONF 94-6. The final result is to be published.
[10] We use $\mathcal{B}(\tau \to \ell\bar{\nu}_\ell\nu_\tau) = (35.31 \pm 0.31)\%$.